CARBON 49 (2011) 3019–3023

available at www.sciencedirect.com

ScienceDirect

journal homepage: www.elsevier.com/locate/carbon

Hydrazine-reduction of graphite- and graphene oxide

Sungjin Park [a,b], *Jinho An* [a], *Jeffrey R. Potts* [a], *Aruna Velamakanni* [a], *Shanthi Murali* [a], *Rodney S. Ruoff* [a,*]

[a] *Department of Mechanical Engineering and the Texas Materials Institute, The University of Texas at Austin, One University Station C2200, Austin, TX 78712-0292, USA*

[b] *Department of Chemistry, Inha University, Incheon 402-751, Republic of Korea*

ARTICLE INFO

Article history:
Received 21 October 2010
Accepted 27 February 2011
Available online 15 March 2011

ABSTRACT

We prepared hydrazine-reduced materials from both graphite oxide (GO) particles, which were not exfoliated, and completely exfoliated individual graphene oxide platelets, and then analyzed their chemical and structural properties by elemental analysis, XPS, TGA, XRD, and SEM. Both reduced materials showed distinctly different chemical and structural properties from one another. While hydrazine reduction of graphene oxide platelets produced agglomerates of exfoliated platelets, the reduction of GO particles produced particles that were not exfoliated. The degree of chemical reduction of reduced GO particles was lower than that of reduced graphene oxide and the BET surface area of reduced GO was much lower than that of reduced graphene oxide.

1. Introduction

Graphene, which has a two dimensional structure consisting of an sp^2 carbon network with a thickness of one atom, is of both fundamental interest and also for a wide range of potential applications due to its excellent mechanical, thermal, and electrical properties [1–6]. The reduction of electrically insulating graphene oxide, which is exfoliated from graphite oxide (GO), and use of the colloidal suspensions of reduced graphene oxide is one of the most promising ways to produce electrically conducting graphene-based platelets on a large scale [7–11], and thus its potential in composites [12–14], paper-like materials and thin films [15,16], as substrates [17,18], as a coating layer [19], and as transparent conductive films [20,21]. Graphene oxide has a wide range of oxygen functionalities, such as 1,2-epoxide and alcohol groups on the basal planes, and carboxyl and ketone groups at the edges [22–25]. It is well-known that significant amounts of these oxygen functional groups are removed by chemical reduction using reductants, producing electrically conducting platelets [26]. In this work, we compare the reduction of individual graphene oxide platelets, which are completely exfoliated, and GO particles, which have not been exfoliated, by hydrazine.

The degree of reduction of graphene oxide will significantly influence the physical properties of chemically reduced graphene oxide materials, and is dependent on reaction conditions. For example, it is known that the carbon to oxygen atomic ratio and electrical conductivity of reduced graphene oxide varies depending on chemical identity of the reductants (such as hydrazine, 1,1-dimethylhydrazine, hydroquinone, and sodium borohydride) [11,12,26,27]. However, the effect of other factors (e.g., particle size of graphite, oxidation methods for preparing GO, reaction temperature, solvents, etc.) on the reduction is of interest. For example, is there a difference in the chemistry of exposure to hydrazine of graphene oxide platelets, which are completely exfoliated, and GO particles, which are not? Oxygen functional groups projecting into the interlamellar spaces between adjacent layers in GO particles may have different reaction environments (perhaps due to steric hindrance) than completely exfoliated graphene oxide platelets. The compliance of almost atom-thick layers is

* *Corresponding author:*
E-mail address: r.ruoff@mail.utexas.edu (R.S. Ruoff).
0008-6223/$ - see front matter
doi:10.1016/j.carbon.2011.02.071

also such that the suspended individual layers (i.e., graphene oxide platelets) are likely not as topologically constrained as the layers present in the GO particles. Such considerations also motivate the work reported here.

2. Experimental

2.1. Sample preparation

2.1.1. Preparation of chemically reduced graphene oxide (CReGO)

GO was synthesized from natural graphite (SP-1, Bay Carbon, MI) by a modified Hummers method [28]. A colloidal suspension of individual graphene oxide platelets in purified water (3 mg/ml) was prepared by sonication of GO in 2 L batches bath ultrasound (VWR B2500A-MT) with 3 h. Hydrazine monohydrate (1 μl for 3 mg of GO, 98%, Aldrich) was subsequently added to the suspension. Additional stirring with a Teflon-coated stirring bar in an oil bath held at 80 °C for 12 h yielded a black precipitation of reduced graphene oxide powder. After cooling to room temperature, the powder was filtered through a fritted glass filter (medium pore size), followed by suction-drying under house-vacuum for 12 h. The resulting black material was dried under vacuum using a mechanical pump.

2.1.2. Preparation of chemically reduced graphite oxide (RGO)

GO powder was added to a flask containing purified water (3 mg/ml). Immediately after addition, hydrazine monohydrate (1 μl for 3 mg of GO) was added to the mixture and the flask was immersed into an oil bath at 80 °C. After additional stirring for 12 h, the resulting black powder was filtered and dried following the same method as for CReGO.

2.2. Characterization

XPS measurements of powder samples were performed with an Omicron ESCA Probe (Omicron Nanotechnology, Taunusstein, Germany) using monochromatic Al-K_α radiation ($h\nu$ = 1486.6 eV). Atlantic Microlab, Inc. (www.atlanticmicrolab.com) did the elemental analysis of the powder samples. Scanning electron microscope (SEM) images were taken by an FEI Quanta-600 FEG Environmental SEM. The thermogravimetric analysis (TGA) of powder samples was measured with a Perkin–Elmer TGA 4000 using a 1°/min heating rate under nitrogen flow (20 ml/min). X-ray diffraction (XRD) of the powder samples was recorded for 2θ values from 10° to 50° in order to characterize the interlayer spacing. The characterization was done in a Phillips powder X-ray diffractometer at 40 keV and 30 mA with a step size of 0.02° and a dwell time of 2.0 s. Samples were mounted using a low melting temperature wax onto a special quartz substrate (cut 6° from (0 0 0 1)) designed to minimize the background signal. BET surface area measurements were done using a Quantachrome Instruments Nova 2000.

3. Results and discussion

In this work, we chemically reduced two samples in water: aqueous slurry containing GO particles, and separately, a homogeneous colloidal suspension of exfoliated graphene oxide platelets, which was generated by simple sonication in water (Fig. 1a and b). To minimize exfoliation of the thin GO platelets in such slurry, hydrazine was added to the flask immediately after the addition of GO particles into the flask filled with the de-ionized water. Each reaction flasks were then separately immersed in an oil bath held at 80 °C, under stirring with a magnetic bar. Among several chemical reductants reported [7,11,12,26,27], we chose hydrazine monohydrate, which is the most frequently used reductant due to its simple reduction procedure and generation of highly reduced graphene oxide with excellent physical properties [9,26,28,29].

Powder samples of chemically reduced graphene oxide (CReGO) and reduced GO (RGO) were both black in color, as is typically observed for reduced graphene/graphite oxide materials. A scanning electron microscope (SEM) image of fluffy CReGO powder shows agglomeration of the exfoliated platelets (Fig. 1c), while that of RGO powders shows thick particles that have not been exfoliated along with outer layers that have slightly delaminated during reduction with stirring (Fig. 1d and e).

Elemental analysis by combustion was used to investigate the degree of reduction of the powder samples. The C/O atomic ratio of GO was ~1.2, which includes the contribution of water molecules trapped in the hydrophilic GO particles. The C/O ratio of CReGO was ~10.2, indicating that many oxygen atoms were removed by the chemical reduction. In contrast, the C/O ratio of RGO (~5.0) suggests that GO particles are reduced by reaction with hydrazine; however, the degree of reduction of RGO was lower than that of CReGO. Additionally, an N component has been found in materials that are produced by reduction of graphene oxide with hydrazine (NH_2NH_2) [26]. Although the chemical structure(s) and reaction mechanism(s) associated with these N species in reduced graphene oxide are not yet understood, it is thought that the N atoms come from hydrazine during reduction. The C/N ratio of CReGO was ~22.7, while that of RGO was ~49.5, indicating that the RGO has fewer N atoms than CReGO and presumably indicating lower degree of reduction of RGO than of CReGO.

Chemical analysis of powder samples of GO, RGO, and CReGO was conducted by X-ray photoelectron spectroscopy (XPS, Fig. 2a). The C1*s* XPS spectrum of GO shows two large peaks at 284.6 eV, corresponding to sp^2 carbon components, and at 286.7 eV, corresponding to C–O single bond components of hydroxyl and 1,2-epoxide functionalities, and shows a broad small shoulder at approximately 288–289 eV, corresponding to C=O double bond components of carboxyl and ketone functionalities [30]. The peaks corresponding to those oxygen functional groups in the spectrum of RGO were significantly decreased by the hydrazine reduction; however, the spectrum still shows small peaks in that region. On the other hand, the spectrum of CReGO indicates a higher degree of removal of oxygen components by the hydrazine reduction than that of RGO. The elemental analysis and XPS spectra suggest that the degree of reduction of RGO is lower than that of CReGO.

Thermogravimetric analysis (TGA, Fig. 2b) graphs show weight profiles of powder samples as variation of temperature

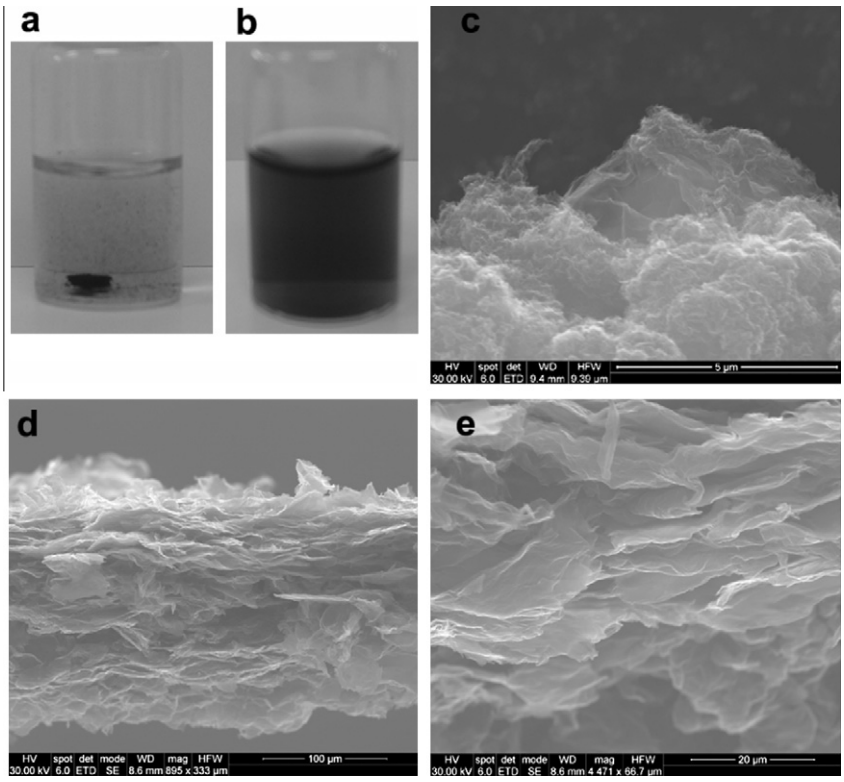

Fig. 1 – Photos of (a) a mixture of graphite oxide particles in water and (b) a homogeneous aqueous colloidal suspension of graphene oxide. SEM images of (c) CReGO and (d), (e) RGO.

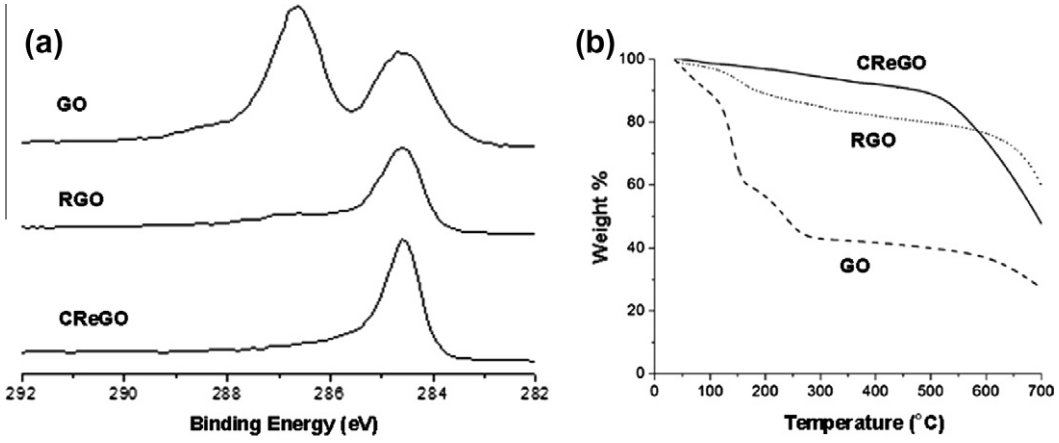

Fig. 2 – (a) C1s XPS spectra and (b) TGA curves of GO, RGO, and CReGO.

(heating rate, 1°/min) under N_2 flow. Weight loss (~11 wt%) of the GO up to 100 °C could be primarily due to evaporation of water molecules held in the samples [26,28]. A comparatively small amount (~1 wt%) of weight loss by CReGO in this temperature region indicates that CReGO does not contain much water as previously reported [26]. In contrast, RGO showed much lower weight loss (~3 wt%) than GO, indicating a less amount of water absorbed by the RGO than by the GO. However, the weight loss is higher than that of CReGO. While GO exhibited significant weight loss (~34 wt%, contributed by combination of evaporation of water and removal of labile oxygen functional groups) [23,26] from 100 to 210 °C, the CReGO lost much less weight (~2 wt%) in this region, suggesting that a significant amount of the water and labile oxygen groups were removed by the hydrazine reduction. Interestingly, the RGO lost approximately 8 wt% in this region, indicating that the RGO was reduced by hydrazine but that the degree of reduction of RGO is lower than that of CReGO.

X-ray diffraction (XRD, Fig. 3) pattern of GO powder shows a larger interlayer spacing than that of graphite (GO, major peak at 10.6° 2θ corresponding to an interlayer spacing of 8.32 Å compared with graphite's major peak from (0 0 2) at 26.53 2θ corresponding to 3.36 Å), due to the oxygen functional groups of GO as well as water molecules held in

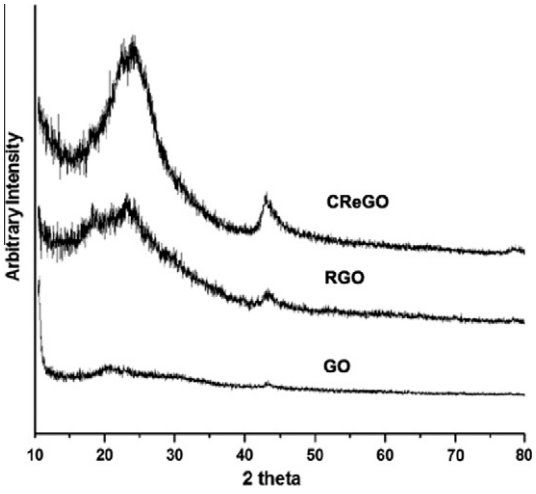

Fig. 3 – XRD patterns of GO, RGO, and CReGO.

the interlayer galleries of hydrophilic GO [31]. In the XRD pattern of CReGO (which is exfoliated into individual platelets and then agglomerated into a powder form), the major peak is observed at about 23–24°. This gives an interlayer spacing of approximately 3.7–3.8 Å. This interlayer spacing is much smaller than the 8.32 Å for GO, and is closer to the (0 0 2) graphite peak of 3.36 Å. The RGO powder shows a broad peak at a similar position to CReGO. Additionally, it has a broad shoulder at $2\theta = 18.5°$ (confirmed by separate measurements of two different RGO batches), presumably induced by a bimodal or multimodal character of the interlayer spacing of RGO powder. The surface area as measured by the BET method (calculated by N_2 gas adsorption on the surface of the materials) of RGO (~82 m^2/g) is much lower than that of CReGO (~487 m^2/g). Since the RGO has largely maintained its layered structure, the surface area of RGO could be much lower than that of CReGO which has been completely exfoliated.

Although the reduction mechanism of RGO is not known with certainty, based on these results we think that the reduction starts from the edges of GO particles and proceeds into the basal planes (Fig. 4). During the reduction, parts of the basal planes near the edges become reduced and subsequently snap together due to π–π interactions, thus narrowing the interlayer distance. Consequently, the reducing agent, hydrazine, cannot penetrate further into the interior of the RGO particles, presumably leading to the lower degree of reduction of RGO relative to CReGO.

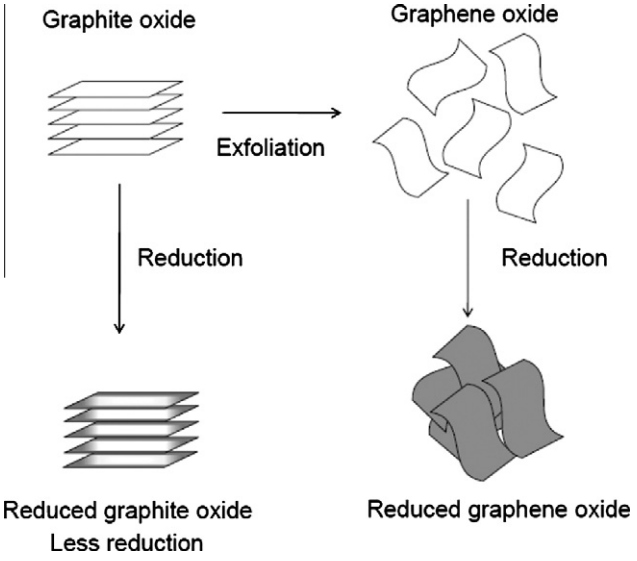

Fig. 4 – Representative scheme to show a degree of reduction of graphite/graphene oxides.

4. Conclusion

We prepared hydrazine-reduced materials from both GO particles, which were not exfoliated, and completely exfoliated individual graphene oxide platelets, and then analyzed their chemical and structural properties by elemental analysis, XPS, TGA, XRD, and SEM. Both reduced materials showed distinctly different chemical and structural properties from one another. While hydrazine reduction of graphene oxide platelets produced agglomerates of exfoliated CReGO platelets, the reduction of GO particles produced RGO particles that were not exfoliated. The degree of chemical reduction of RGO particles was lower than that of CReGO and the BET surface area of RGO was much lower than that of CReGO. We believe that this information will be useful to further understand properties of chemically reduced graphene oxide materials and to help developing consistent methods to produce these materials.

Acknowledgement

S.P. appreciates support from Inha University Research Grant (INHA-42155).

REFERENCES

[1] Geim AK, Novoselov KS. The rise of graphene. Nat Mater 2007;6:183–91.
[2] Lee C, Wei X, Kysar JW, Hone J. Measurement of the elastic properties and intrinsic strength of monolayer graphene. Science 2008;321:385–8.
[3] Seol JH, Jo I, Moore AL, Lindsay L, Aitken ZH, Pettes MT, et al. Two-dimensional phonon transport in supported graphene. Science 2010;328:213–6.
[4] Berger C, Song Z, Li X, Wu X, Brown N, Naud C, et al. Electronic confinement and coherence in patterned epitaxial graphene. Science 2006;312:1191–6.
[5] Rao CNR, Sood AK, Subrahmanyam KS, Govindaraj A. Graphene: the new two-dimensional nanomaterial. Angew Chem Int Ed 2009;48:7752–77.
[6] Rao CNR, Sood AK, Voggu R, Subrahmanyam KS. Some novel attributes of graphene. J Phys Chem Lett 2010;1:572–80.
[7] Park S, Ruoff RS. Chemical methods for the production of graphenes. Nat Nanotechnol 2009;4:217–24.
[8] Li X, Zhang G, Bai X, Sun X, Wang X, Wang E, et al. Highly conducting graphene sheets and Langmuir–Blodgett films. Nat Nanotechnol 2008;3:538–42.
[9] Park S, An J, Jung I, Piner RD, An SJ, Li X, et al. Colloidal suspensions of highly reduced graphene oxide in a wide variety of organic solvents. Nano Lett 2009;9(4):1593–7.

[10] Niyogi S, Bekyarova E, Itkis ME, L MJ, Hamon MA, Haddon RC. Solution properties of graphite and graphene. J Am Chem Soc 2006;128:7720–1.
[11] Si Y, Samulski ET. Synthesis of water soluble graphene. Nano Lett 2008;8(6):1679–82.
[12] Stankovich S, Dikin DA, Dommett GHB, Kohlhaas KM, J ZE, Stach EA, et al. Graphene-based composite materials. Nature 2006;442:282–6.
[13] Wang H, Hao Q, Yang X, Lu L, Wang X. Effect of graphene oxide on the properties of its composite with polyaniline. ACS Appl Mater Interfaces 2010;2:821–8.
[14] Liang J, Huang Y, Zhang L, Wang Y, Ma Y, Guo T, et al. Molecular-level dispersion of graphene into poly(vinyl alcohol) and effective reinforcement of their nanocomposites. Adv Func Mater 2009;19:2297–302.
[15] Dikin DA, Stankovich S, Zimney EJ, Piner R, Dommett GHB, Evmenenko G, et al. Preparation and characterization of graphene oxide paper. Nature 2007;448:457–60.
[16] Chen H, Muller MB, Gilmore KJ, Wallace GG, Li D. Mechanically strong, electrically conductive, and biocompatible graphene paper. Adv Mater 2008;20:3557–61.
[17] Lee DH, Kim JE, Han TH, Hwang JW, Jeon S, Choi S-Y, et al. Versatile carbon hybrid films composed of vertical carbon nanotubes grown on mechanically compliant graphene films. Adv Mater 2010;22(11):1247–52.
[18] Kim BH, Kim JY, Jeong S-J, Hwang JO, Lee DH, Shin DO, et al. Surface energy modification by spin-cast, large-area graphene film for block copolymer lithography. ACS Nano 2010;4:5464–70.
[19] Han TH, Lee WJ, Lee DH, Kim JE, Choi E-Y, Kim SO. Peptide/graphene hybrid assembly into core/shell nanowires. Adv Mater 2010;22(18):2060–4.
[20] Watcharotone S, Dikin DA, Stankovich S, Piner R, Jung I, Dommett GHB, et al. Graphene–silica composite thin films as transparent conductors. Nano Lett 2007;7:1888–92.
[21] Eda G, Fanchini G, Chhowalla M. Large-area ultrathin films of reduced graphene oxide as a transparent and flexible electronic material. Nat Nanotechnol 2008;3:270–4.
[22] Cai W, Piner RD, Stadermann FJ, Park S, Shaibat MA, Ishii Y, et al. Synthesis and solid-state nmr structural characterization of ^{13}C-labeled graphite oxide. Science 2008;321:1815–7.
[23] Lerf A, He H, Forster M, Klinowski J. Structure of graphite oxide revisited. J Phys Chem B 1998;102(23):4477–82.
[24] He H, Klinowski J, Forster M, Lerf A. A new structural model for graphite oxide. Chem Phys Lett 1998;287:53–6.
[25] He H, Riedl T, Lerf A, Klinowski J. Solid-state NMR studies of the structure of graphite oxide. J Phys Chem 1996;100:19954–8.
[26] Stankovich S, Dikin DA, Piner R, Kohlhaas KM, Kleinhammes A, Jia Y, et al. Synthesis of graphene-based nanosheets via chemical reduction of exfoliated graphite oxide. Carbon 2007;45:1558–65.
[27] Wang G, Yang J, Park J, Wang B, Liu H, Yao J. Facile synthesis and characterization of graphene nanosheets. J Phys Chem C 2008;112:8192–5.
[28] Park S, An J, Piner RD, Jung I, Yang D, Velamakanni A, et al. Aqueous suspension and characterization of chemically modified graphene sheets. Chem Mater 2008;20:6592–4.
[29] Li D, Muller MB, Gilje S, Kaner RB, Wallace GG. Processable aqueous dispersions of graphene nanosheets. Nat Nanotechnol 2008;3:101–5.
[30] Park S, Lee K-S, Bozoklu G, Cai W, Nguyen ST, Ruoff RS. Graphene oxide papers modified by divalent ions – Enhancing mechanical properties via chemical cross-linking. ACS Nano 2008;2(3):572–8.
[31] Buchsteiner A, Lerf A, Pieper J. Water dynamics in graphite oxide investigated with neutron scattering. J Phys Chem B 2006;110:22328–38.